

Design and Study of Fractal Optical Modulator for Infrared Transmitted Signal

A. A. Shehab, A. A. Mohammad*, and A. R. Salihand
College of Education Ibn Al-Haitham, University of Baghdad,

***Laser and Optoelectronics Engineering, University of Technology**

Abstract

The optical modulator was designed by using iterated function systems (IFSs) by IFS Construction Kit program. The modulator was inserted into the optical system using ZEMAX optical design program. In this program, it is assumed that the modulator is made from one of the infrared transmitting materials. Eight materials at room temperature were used in this study; these are IRTRAN materials, Si, and Ge for the range of 3-9 μm .

Systems were evaluated and analyzed by using different criteria, including spot diagram, modulation transfer function, and point spread function. The effect of optical modulator change with the change of its material results in focusing of functions and frequencies as required. Root mean square and geometrical spot sizes decrease with the increase of the refractive index, while the maximum spatial frequency increases.

Introduction

Classical geometry defines the basic shapes such as points, lines, and circles. Much of the universe around us can be explained and understood by using those classical constructions. However, there are many objects in nature that cannot be represented with these simple shapes. For example, a mountain is not just a cone. There are smaller peaks and valleys of all sizes on the surface of the mountain that make it distinctly different from any simple shape. The shape of a mountain and other natural objects can be described through something which is called a fractal. A fractal is any object that exhibits self-similarity. Self-similarity means that any small part of the object always looks

like a small copy of the whole object. The small peaks and valleys on the surface of a mountain, often look like small copies of the mountain itself (1).

An optical modulator (a reticle or a chopper) is used to provide directional information for tracking and to suppress unwanted signals from backgrounds. The optical modulator can assume many forms, but basically each can be described as a pattern of alternately clear and opaque areas carried on a suitably transparent substrate (Fig.1).

The infrared (IR) is often subdivided into four regions: the near IR (NIR) (0.75-3 μm), the middle IR (MIR) (3-6 μm), the far IR (FIR) (6-15 μm), and the extreme IR (XIR) (15-1000 μm) (2). There are three main windows in the atmosphere; one from 0.75-2.5 μm (NIR), another from 3-5 μm (MIR), and a third from 7.5-14 μm (FIR) (3).

IRTRAN 1-6 materials are fabricated from hot pressed MgF_2 , ZnS , CaF_2 , ZnSe , MgO , and CdTe , respectively. These polycrystalline materials are developed by the Eastman Kodak Company of Rochester, New York (2).

Generally the requirements for infrared transmitting materials are set primarily by the atmospheric transmission and secondarily by the operational wavelength range of the sources and detectors and by the power handling requirements of particular systems (3).

Theoretical Background

Fractals reproducing realistic shapes, such as mountains, clouds, or plants, can be generated by the iteration of one or more affine transformations. An affine transformation is a recursive transformation of the type

$$\begin{pmatrix} x_{n+1} \\ y_{n+1} \end{pmatrix} = \begin{pmatrix} a & b \\ c & d \end{pmatrix} \begin{pmatrix} x_n \\ y_n \end{pmatrix} + \begin{pmatrix} e \\ f \end{pmatrix} \quad [1]$$

Each affine transformation will generally yield a new attractor in the final image. The form of the attractor is given through the choice of the coefficients a , b , c , d , e , and f , which uniquely determine the affine transformation. To get a desired shape, the collage of several attractors (i.e. several affine transformations) may be used. This method is referred to as an iterated function system (IFS) (4).

In any optical material, the spectral variation of the refractive index is determined experimentally. However, often it is convenient to

have an analytical approximation to work with. In the infrared spectrum, the Herzberger formula is mainly used:

$$n = A + BL + CL^2 + D\lambda^2 + E\lambda^4, L = (\lambda^2 - 0.028)^{-1} \quad [2]$$

where n is the refractive index at wavelength λ , and the other symbols are constants determined experimentally. Table 1 lists the appropriate constants for the materials in this study. Also the spectral range of validity is given (5).

To the system which engineers the purpose of the optics in its infrared system, it is to collect a radiant flux and deliver it to the detector which converts it into an electrical signal Fig. (2). Before reaching the detector, the radiation from the target may pass through an optical modulator where it is coded with information concerning the direction to the target or information to assist in the differentiation of the target from unwanted details in the background. The electrical signal from the detector passes to the processor where it is amplified and the coded target information is extracted. The final step is the use of this information to automatically control some process or to display the information for interpretation by a human observer.

The reticle is, in effect, a selective modulator that is most efficient against point-source targets. For the highest modulation efficiency, the openings in the reticle should match the size of the target image. In practical designs they may be up to three times as large as the size of the image. Since the openings in the reticle are of approximately the same size as the image of the target, the electrical signal from the detector is a series of pulses at the chopping frequency f_c .

$$f_c = mf_r \quad [3]$$

where m is the number of pairs of clear and opaque segments in the reticle and f_r is its rotational frequency expressed in revolutions per second. In Fig. 2, the chopped target signal is shown as a series of square pulses. It will be realized that the exact shape of the pulses depends on the relative sizes of the image and the openings in the reticle, as well as the manner in which the signal is modified by subsequent signal processing circuitry.

Reduced to its basic elements, any optical system consists of one or more reflecting or refracting elements. All elements are considered to be centered; that is, the centers of curvature of each of the surfaces all lie on the same straight line, called the optical axis.

Any departure from this condition because of poor manufacturing or careless mounting impairs the performance of the optics.

In considering the amount of radiant flux collected by an optical system, it is important to know the diameter of the largest bundle of rays that can pass through the optics without obstruction. The physical object that limits this bundle is called the aperture stop. Should there be optical elements in front of the aperture stop, the image of the stop that they form is called the entrance pupil.

There are two important ways of describing the amount of radiant flux collected by an optical system. The first uses the $f / \#$ number of the optics

$$f / \# = \frac{f}{D} \quad [4]$$

where f is the effective focal length and D is the diameter of the aperture stop or entrance pupil (2). Working $f / \#$ is defined as

$$Wf / \# = \frac{1}{2n' \sin \varphi_r} \quad [5]$$

where φ_r is the real marginal ray angle in the image space and n' is the refractive index of the image space. The paraxial working $f / \#$ is defined as

$$PWf / \# = \frac{1}{2n' \tan \varphi_p} \quad [6]$$

where φ_p is the paraxial marginal ray angle in the image space (9).

An alternative means of describing flux collection is the numerical aperture, which is given by

$$NA = n'' \sin u \quad [7]$$

where n'' is the refractive index of the medium between the final optical surface and the second focal point, and u is the half-angle of the cone of rays converging at the focal point. The relationship between the numerical aperture and $f / \#$ number is

$$NA = \frac{1}{2(f / \#)} \quad [8]$$

The image of a point source formed by diffraction-limited (aberration free) optics appears as a bright central disk surrounded by several alternately bright and dark rings. The central disk contains 84% of the radiant flux, and the rest is in the surrounding rings. Since

Airy was one of the first to analyze the diffraction process, the central disk is usually called the Airy disk. The linear diameter of this disk, which is considered to be equal to the diameter of the first dark ring, is

$$d_A = (2.44\lambda)(f/\#) \quad [9]$$

where d_A and λ are both expressed in micrometers (2).

The optical transfer function (OTF) of an optical system is a spatial-frequency dependent complex quantity whose modulus is the modulation transfer function (MTF) and whose phase is the phase transfer function (PTF). The former is a measure of the reduction in contrast from an object to an image over the spectrum. The latter represents the commensurate relative phase shift. Phase shifts in centered optical systems occur only off axis and often the PTF is of less interest than the MTF (10). The MTF describes the ability of a system element, or of an entire system, to transfer information. It is of a particular value because, at least in theory, the transfer functions of each system element may be multiplied together to give the MTF for the entire system (2). The point spread function $\delta(Y, Z)$ (Fig. 3) characterizes the imaging performance of an optical system in its image plane Σ_i , for a point object. If the geometrical aberrations vanish completely, then only diffraction determines the nature of the point spread function (PSF) (11).

Results and Discussion

To construct any fractal by IFS Construction Kit program, there are seven required coefficients for each function. These coefficients are shown in Table 2 for an optical modulator which has ten opaque and ten transparent sectors (Fig. 4). It is constructed through the use of ten affine transformations (with weighted probabilities).

There are many optical design softwares such as ZEMAX, ATMOS, OpTaliX, CODE V, and others. In this work, ZEMAX program were used.

Firstly, data in Table 1 must be used to define the materials into ZEMAX program.

In this study, an entrance pupil diameter of 2.9 mm , one field angle of zero , and five wavelengths (3-5, 8, and 9 μm) have been used .

Table (3) shows data editor for a system without reticle. General data of this system are listed in Table 4 and its two-dimensions layout is shown in Fig. (5).

This system and those to follow, can be analyzed by several different criteria, such as spot diagram, MTF, and PSF. For this system, spot diagram is shown in Fig. 6, MTF is in Fig. 7, and PSF in Fig. 8. The general tendency of MTF curves is that higher spatial frequencies mean lower MTF values. In MTF plots, $MTF = 1$ at zero spatial frequency and $MTF = 0$ near and at maximum spatial frequency.

Table (5) shows data editors when the reticle is added. The general data are listed in Table 6. Now, this system (Fig. 9) is similar to that shown in Fig. (2).

Table (7) shows the differences in systems 2-9. Every property in this table will either decrease or increase with increasing refractive index of the reticle material. From this table the following can be observed:

1. All materials which were studied showed a small change in the effective and back focal lengths with the changing reticle material, i.e. with changing refractive index and this change does not affect focusing.
2. Changing refractive index results in no appreciable change of $f/\#$ or NA . This change is insignificant in this work. Working $f/\#$ is greater than the paraxial working $f/\#$ (i.e. $\varphi_r < \varphi_p$).
3. Increasing the refractive index would cause a small increase in stop radius.
4. Entrance pupil position decreases clearly with the increase of the refractive index, while exit pupil diameter increases by a small value. This is due to the change in refractive angles of rays through system material.
5. Root mean square (RMS) and geometrical (GEO) spot sizes decrease when the refractive index is increased because of the change in the refractive angles of rays with the refractive index. Diameter of the Airy disk decreases with the increase refractive index.
6. The effect of the increase in refractive index is to increase the maximum spatial frequency.

7. Side (in PSF figure) decreases with the increase of the refractive index.

The MTF of the fractal (Fig. 4) and that of the optical design (Fig. 9) may be multiplied together to give the total MTF, i.e.

$$(MTF)_{tot} = (MTF)_{fra} \cdot (MTF)_{opt}$$

In this study, it is assumed that $(MTF)_{fra}$ has a value of unity for all spatial frequencies (i.e. perfect MTF) so that the total MTF is that of Fig. 9.

Conclusions

From the results, the following conclusions can be drawn:

1. The variation of the optical modulator material indicates that the refractive index is associated with spot sizes, functions, and frequencies.
2. If the size of the smallest detector available is $50 \mu\text{m}$, the step to take is to use systems 2-9 at a wavelength larger than $5 \mu\text{m}$ or to decrease temperature in order to insure that the size of the image is smaller than the size of the detector (i.e. the diameter of the Airy disk is larger than the size of the detector).
3. ZEMAX program can be used to design systems which contain optical modulator.

References

1. Al-Rammahi, A. M. H. R. (2005). Linear and Non-linear Fractal Interpolating Functions. Ph.D. Thesis, University of Technology.
2. Hudson, R. D., Jr. (1969). Infrared System Engineering. New York: Wiley.
3. Savage, J. A. (1985). Infrared Optical Materials and their Antireflection Coatings. Bristol: Adam Hilger.
4. Bradley, L. D. (2007). Iterated Function Systems, www.pha.jhu.edu/~ldb/seminar/ifs.html.
5. Levi, L. (1980). Applied Optics: A Guide to Optical System Design, Vol. 2. New York: Wiley.
6. Eastman-Kodak Co. (1971). Publ. No. U-72.
7. Edwards, D. F. and E. Ochoa (1980). Infrared Refractive Index of Silicon. Appl. Opt., 19, 4130-4131.

8. Herzberger, M. and C. D. Salzberg (1962). Refractive Indices of Infrared Optical Materials and Color-Correction of Infrared Lenses. *J. Opt. Soc. Am.*, 52, 420-427.
9. ZEMAX Optical Design Program: User's Guide (2007), www.zemax.com.
10. Hecht, E. and A. Zajac (1974). *Optics*. Reading, Mass.: Addison-Wesley.
11. Stoltzmann, D. E. (1983). *Applied Optics and Optical Engineering*, Vol. IX, ed. by R. R. Shannon and J. C. Wyant. New York: Academic Press.

Table (1): Data for Herzberger's dispersion formula for eight optical materials at room temperature. Data for IRTRAN materials are taken from (6).

Material	Spectral Range (μm)	A	B	C	D	E
IRTRAN-1	0.5-9	1.3776955	0.0013515529	2.1254394×10^{-4}	$-1.5041172 \times 10^{-3}$	$-4.4109708 \times 10^{-6}$
IRTRAN-3	0.5-11	1.4278071	0.0022806966	$-9.1939015 \times 10^{-5}$	$-1.1165792 \times 10^{-3}$	$-1.5949659 \times 10^{-6}$
IRTRAN-5	0.5-9	1.7200516	0.00561194	$-1.0986148 \times 10^{-5}$	$-3.0994558 \times 10^{-3}$	$-9.6139613 \times 10^{-6}$
IRTRAN-2	0.5-13	2.2569735	0.032640935	6.0314637×10^{-4}	$-5.2705532 \times 10^{-4}$	$-6.0428638 \times 10^{-7}$
IRTRAN-4	0.5-20	2.4350823	0.051567572	2.4901923×10^{-3}	$-2.7245212 \times 10^{-4}$	$-9.8541275 \times 10^{-8}$
IRTRAN-6	0.9-16	2.682384	0.118029	0.03276801	-1.202984×10^{-4}	2.177336×10^{-8}
Si (7)	2.4-25	3.41983	0.159906	-0.123109	1.26878×10^{-6}	-1.95104×10^{-9}
Ge(8)	2-13.5	3.99931	0.391707	0.163492	-6×10^{-6}	5.3×10^{-8}

Table (2): IFS codes of fractal optical modulator.

	Matrix				Translation		Probability
	a	b	c	d	e	f	
1	0.050	0.002	-0.030	0.344	290.000	10.000	0.092
2	0.050	0.002	0.030	0.305	295.000	320.000	0.091
3	0.050	0.250	0.050	-0.300	340.000	160.000	0.091
4	-0.020	0.250	0.050	0.250	346.000	297.000	0.139
5	0.050	-0.400	-0.030	-0.100	210.000	230.000	0.114
6	0.050	0.380	0.065	0.100	360.000	250.000	0.086
7	-0.020	-0.300	-0.055	0.250	220.000	280.000	0.068
8	0.050	0.400	0.050	-0.150	360.000	212.000	0.091
9	0.050	-0.150	0.010	0.305	240.000	310.000	0.114
10	0.050	-0.300	-0.030	-0.305	235.000	177.000	0.114
							1.000

521.380	Fractal Space	358.475	Design Space
y max		y max	
-52.582		y min	
11.269	585.230	-18.926	378.525
x min	x max	x min	x max

Table (3): Data editor of system 1.

Surf:Type	Radius	Thickness	Glass	Semi-Diameter
OBJ	Standard	Infinity		0.000000
1	Standard	Infinity	IRTRAN-2	1.600000 U
2	Standard	-11.800000		1.500000 U
STO	Standard	5.000000	IRTRAN-3	1.100000 U
4	Standard	-14.800000		1.050000 U
IHA	Standard	Infinity		1.600000 U

Table (4): General data of system 1.

Effective Focal Length (in air or in image space)	9.051101
Back Focal Length	0.1710887
Image Space $f / \#$ (=Paraxial Working $f / \#$)	3.121069
Working $f / \#$	3.192604
Image (IMA) Space NA	0.1581845
Object (OBJ) Space NA	1.45e-010
Stop(STO) Radius	0.06114088
Entrance Pupil Position	213.5301
Exit Pupil Diameter	0.1230167
Exit Pupil Position	-2.912855
Glass Catalogs	Infrared
Ray Aiming	Off
Apodization	Uniform, factor = 0.00000E+000
Paraxial Image Height	0
Paraxial Magnification	0
Angular Magnification	0

Table (5): Data editors of systems 2-9.

Surf	Type	Radius	Thickness	Class	Semi-Diameter
OBJ	Standard	Infinity	Infinity		0.000000
1	Standard	Infinity	0.200000	IRTRAN-2	1.600000 U
2	Standard	-11.800000	9.000000		1.500000 U
3	Standard	Infinity	0.100000	MATERIAL	1.500000 U
STO	Standard	Infinity	2.000000		1.100000 U
5	Standard	5.000000	0.300000	IRTRAN-3	1.100000 U
6	Standard	-14.800000	2.700000		1.050000 U
IMA	Standard	Infinity			1.800000 U

Table (6) General data of systems 2-9.

System	System 2	System 3	System 4	System 5	System 6	System 7	System 8	System 9
Effective Focal Length (in air or in image space)	11.63843	11.63396	11.61567	11.59211	11.58683	11.58062	11.56792	11.56098
Back Focal Length	-2.302668	-2.298391	-2.280902	-2.258373	-2.253324	-2.247392	-2.235245	-2.22861
Image Space f / # (= Paraxial Working f / #)	4.013253	4.011711	4.005403	3.997278	3.995457	3.993318	3.988937	3.986544
Working f / #	4.192322	4.190524	4.183201	4.173827	4.171733	4.169277	4.164256	4.161518
Image Space NA	0.1236314	0.1236782	0.12387	0.1241179	0.1241736	0.1242391	0.1243734	0.1244469
Stop Radius	0.04982689	0.0502572	0.05202047	0.05430003	0.05481224	0.05541452	0.05664986	0.05732581
Entrance Pupil Position	264.129	261.7878	252.5988	241.6038	239.2591	236.5575	231.196	228.3601
Exit Pupil Diameter	0.1291854	0.1303011	0.1348727	0.1407828	0.1421108	0.1436724	0.1468752	0.1486277
Exit Pupil Position	-5.521121	-5.521121	-5.521121	-5.521121	-5.521121	-5.521121	-5.521121	-5.521121

The others remain the same as in Table 4.

Table (7): Systems have reticle made of infrared material

System	System 2	System 3	System 4	System 5	System 6	System 7	System 8	System 9
Reticle Material	IRTRAN-1	IRTRAN-3	IRTRAN-5	IRTRAN-2	IRTRAN-4	IRTRAN-6	Si	Ge
Effective Focal Length (mm) (in air or in image space)	11.63843	11.63396	11.61567	11.59211	11.58683	11.58062	11.56792	11.56098
Back Focal Length (mm)	-2.302668	-2.298391	-2.280902	-2.258373	-2.253324	-2.247392	-2.235245	-2.22861
Image Space f / # (= Paraxial Working f / #)	4.013253	4.011711	4.005403	3.997278	3.995457	3.993318	3.988937	3.986544
Working f / #	4.192322	4.190524	4.183201	4.173827	4.171733	4.169277	4.164256	4.161518
Image Space NA	0.1236314	0.1236782	0.12387	0.1241179	0.1241736	0.1242391	0.1243734	0.1244469
Stop Radius (mm)	0.04982689	0.0502572	0.0520204	0.0543000	0.0548122	0.0554145	0.0566498	0.0573258
Entrance Pupil Position (mm)	264.129	261.7878	252.5988	241.6038	239.2591	236.5575	231.196	228.3601
Exit Pupil Diameter (mm)	0.1291854	0.1303011	0.1348727	0.1407828	0.1421108	0.1436724	0.1468752	0.1486277
Spot Diagram	493.105	492.767	492.041	490.466	490.177	489.852	489.186	488.833
RMS Radius (μ m)	677.500	677.200	675.978	674.406	674.054	673.641	672.794	672.332
GEO Radius (μ m)	30.69	30.67	30.62	30.55	30.54	30.52	30.48	30.46
Airy Diameter (μ m)	85.02	85.08	85.12	85.35	85.39	85.42	85.50	85.54
Maximum Spatial Frequency (c / mm)	386.84	386.67	386.00	385.13	384.94	384.71	384.25	384.00
Side (μ m)								



Fig. (1): Optical modulator

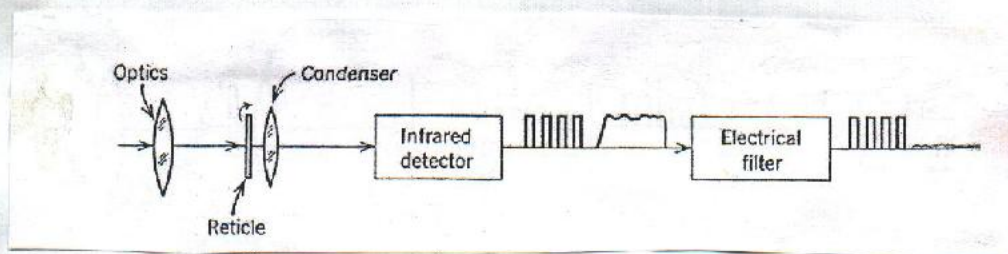


Fig. (2) Reticle system (2)

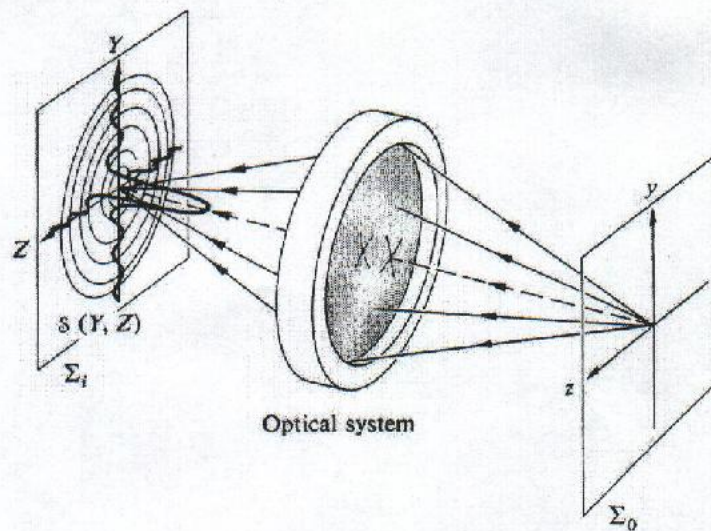


Fig.(3)The point spread function (10)

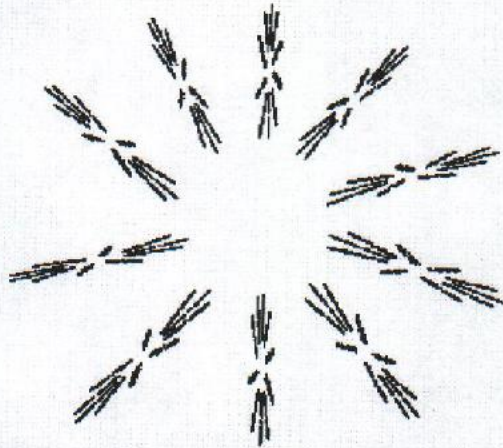


Fig.(4) Fractal optical modulator

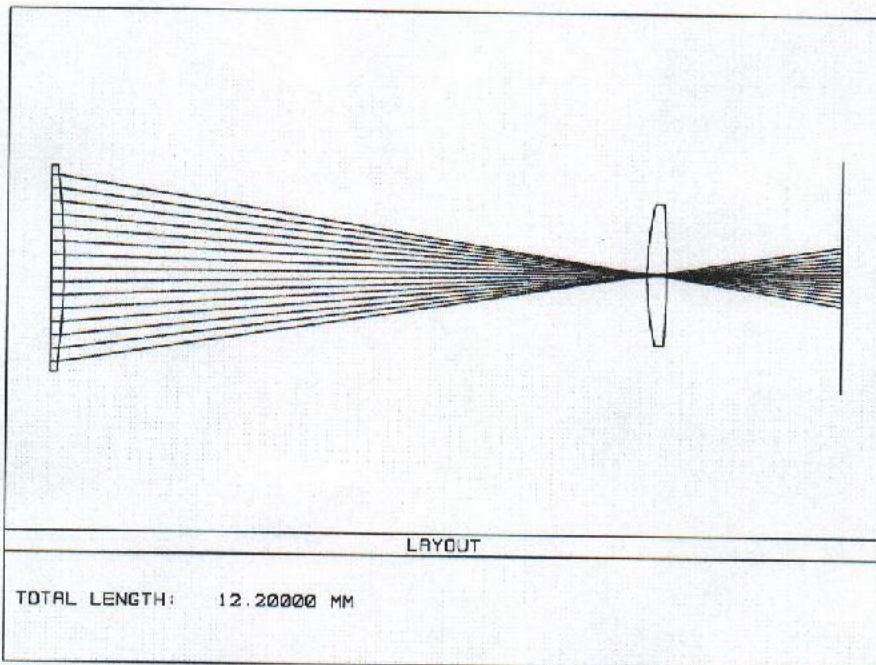


Fig. (5) Layout of system 1

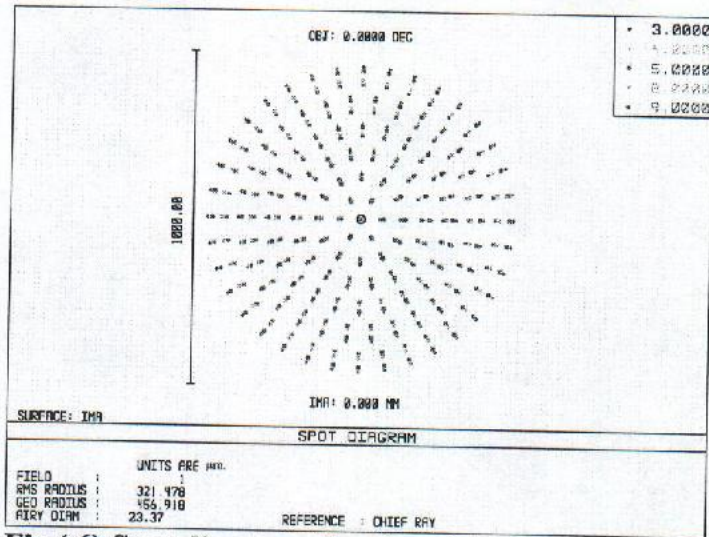


Fig.(6) Spot diagram of system 1

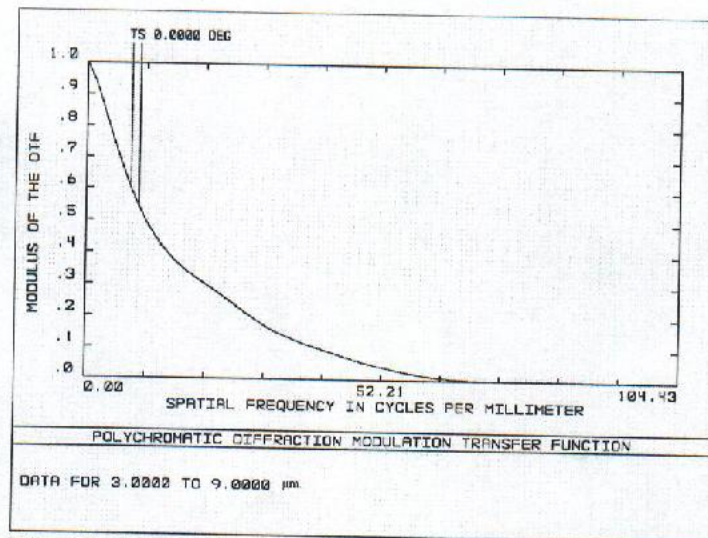


Fig.(7) MTF of system 1

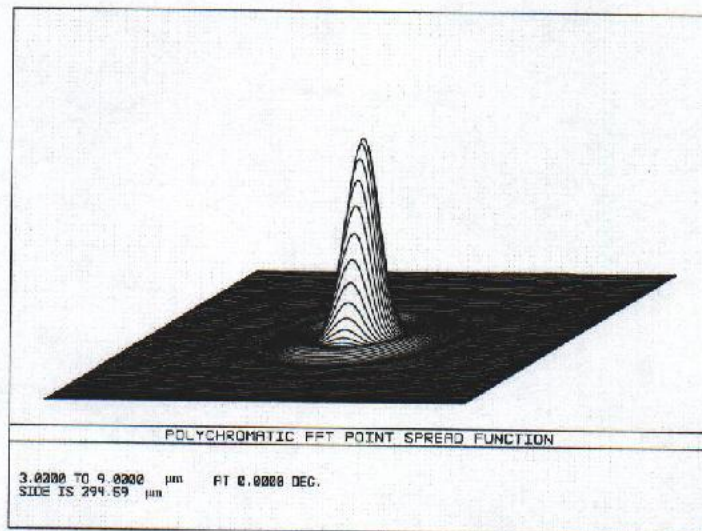


Fig.(8) Fast Fourier Transform (FFT) PSF of system 1

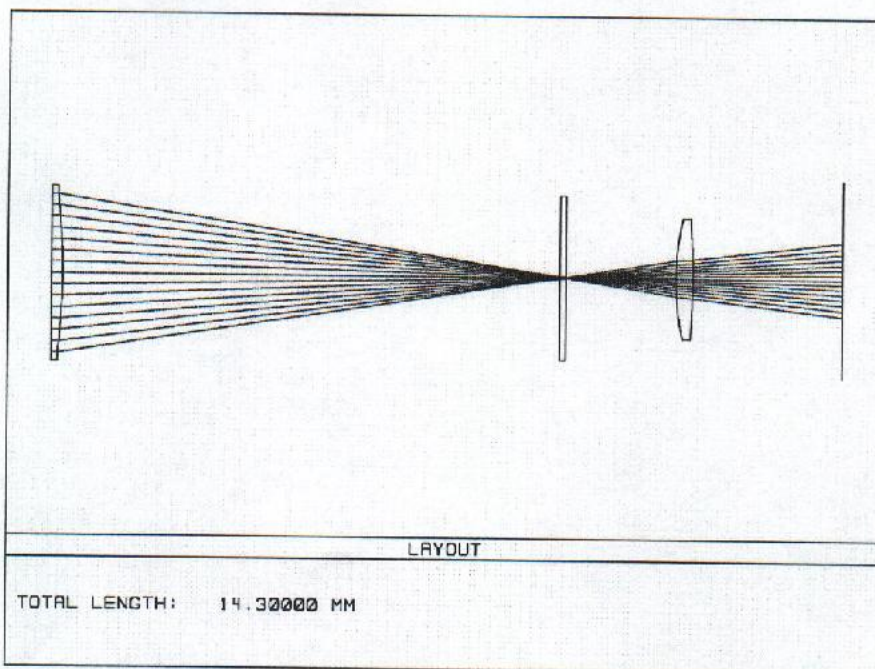


Fig.(9) Layout of systems 2-9

تصميم و دراسة مضمن بصري كسوري لإشارة تحت الحمراء النافذة

علية عبد المحسن شهاب ، عبد الرزاق عبد السلام محمد* وعقيل رزاق
صالح

كلية التربية ابن الهيثم ، جامعة بغداد

* قسم هندسة الليزر و البصريات الألكترونية، الجامعة التكنولوجية

الخلاصة

صُمم المضمن البصري بإستعمال أنظمة الدالة التكرارية (IFSs) بوساطة برنامج (IFS Construction Kit). أدخل المضمن إلى المنظومة البصرية بإستعمال برنامج التصميم البصري (ZEMAX). أفترض في هذا البرنامج إن المضمن مصنوع من إحدى المواد المنفذة للأشعة تحت الحمراء. أستعملت ثمان مواد عند درجة حرارة الغرفة في هذه الدراسة؛ وهي مواد IRTRAN والسليكون والجرمانيوم للمدى $3-9 \mu\text{m}$. قِيمت الأنظمة وحُللت بإستعمال معايير مختلفة، تضمنت مخطط البقعة، دالة الإنتقال التضمينية ، دالة الإنتشار النقطية. يتغير تأثير المضمن البصري بتغيير مادته ويؤدي ذلك إلى تركيز الدوال والترددات كما هو مطلوب. يتناقص جذر معدل مربع حجم البقعة وحجم البقعة الهندسي بزيادة معامل الإنكسار، بينما يزداد التردد الفضائي الأقصى.